AIChE

Analysis of CO_2 Sorption/Desorption Kinetic Behaviors and Reaction Mechanisms on Li_4SiO_4

Zhang Qi, Han Daying, Liu Yang, Ye Qian, and Zhu Zibin
Dept. of Chemical Engineering, East China University of Science and Technology, Shanghai 200237, China

DOI 10.1002/aic.13861
Published online June 15, 2012 in Wiley Online Library (wileyonlinelibrary.com).

The CO_2 sorption/desorption kinetic behaviors on Li_4SiO_4 were analyzed. The theoretical compositions of the sorption/desorption reactions were calculated using FactSage. The sorption/desorption process on Li_4SiO_4 was investigated by comparing the shrinking core, double exponential, and Avrami–Erofeev models. The Avrami–Erofeev model fits the kinetic thermogravimetric experimental data well and, together with the double-shell mechanism, clearly explains the sorption/desorption mechanism. The sorption process is limited by the rate of the formation and growth of the crystals with double-shell structure consisting of Li_2CO_3 and Li_2SiO_3. The whole desorption process is found to be controlled by the rate of the formation and growth of the Li_4SiO_4 crystals. Furthermore, the influence of steam on the CO_2 sorption process was analyzed. It has been observed that the presence of steam enhance the mobility of Li and, therefore, the rate of diffusion control stage. © 2012 American Institute of Chemical Engineers *AIChE J,* 59: 901–911, 2013
Keywords: CO_2 sorption/desorption process, Li_4SiO_4, kinetic model, steam

Introduction

The greenhouse effect and energy crisis are currently two of the most important problems worldwide. Hence, CO_2 capture technologies are required to decrease CO_2 emissions to the atmosphere and improve energy efficiency. They can be used in the direct separation of CO_2 from the high-temperature exhaust gases from power plants,[1,2] particularly in *in situ* CO_2 sorption-enhanced fuel steam reforming processes, which aims to produce pure hydrogen at lower temperature.[3–6] The key point of a CO_2 sorption-enhanced reaction system is to develop a satisfactory solid CO_2 captor with a large capacity, high selectivity, good cycle performance, and proper kinetic behaviors at relatively high temperatures. Thus far, several materials,[2,7–9] such as hydrotalcite-like materials, CaO-based sorbents, and lithium-containing materials, have been proposed for CO_2 capture. Among these materials, lithium orthosilicate (Li_4SiO_4) is considered to be one of the most potential materials. Li_4SiO_4 has been reported to adsorb CO_2 more than 30 times faster than Li_2ZrO_3 and is lighter and cheaper than Li_2ZrO_3. The mass uptake on Li_4SiO_4 due to CO_2 adsorption is almost 50% greater than the weight change for Li_2ZrO_3.[1] It has also been used in sorption-enhanced fuel steam reforming experiments, where it has shown an evidently promoting effect on the process.[10–12]

Furthermore, in the methane steam reforming system, the existence of H_2O cannot be ignored. Thus, the effect of water on the CO_2 sorption properties is very important for the application of the sorbents. Essaki et al.[13] observed a beneficial effect of adding water when absorbing CO_2 on Li_4SiO_4 at room temperature. Ochoa-Fernández et al.[14] also investigated the CO_2 uptake profiles over Li_4SiO_4 and Li_2ZrO_3 at 525°C and 10% of CO_2 with and without water addition.[14] They also found the same trends of the positive impact of steam on the capture kinetics. These results make Li_4SiO_4 to be more practical in sorption-enhanced steam reforming system. However, the reasons for the beneficial effect of steam addition on the CO_2 absorption kinetics of the CO_2 acceptors are not clear yet. These important phenomena need to be explained by kinetic mechanism.

Meanwhile, the investigation of the reaction system mechanism and design requires a suitable kinetic model for the CO_2 sorption/desorption process in Li_4SiO_4. However, only a few studies have reported relative models for Li_4SiO_4.

Table 1 summarizes the commonly reported models for the sorption processes in different sorbents. The power law model is widely used for CO_2 sorption processes because of its simplicity. Ochoa-Fernández et al.[15] proposed a power law model combined with CO_2 partial pressure to analyze the CO_2 sorption process on Li_2ZrO_3 at 550–600°C. Lee et al.[16] reported a similar model independent of the CO_2 partial pressure in the sorption process on CaO at 650–750°C. The experimental data agree with both of the models well. For a rather narrow temperature range, Rusten reported that the shrinking core model (SCM) is suitable for nonporous solids. However, it did not fit well their experimental data on Li_4SiO_4. Thus, a power law model based on SCM with an exponential factor of 2 combined with CO_2 partial pressure was proposed to fit the experimental data at 530–575°C and was used to simulate the sorption-enhanced fuel steam reforming process.[17]

To investigate the reaction mechanism of the sorption process, Pfeiffer et al.[18,19] proposed a double exponential model

Correspondence concerning this article should be addressed to Zhang Q. at doraqi@hotmail.com.

Table 1. Kinetic Models for the CO_2 Sorption Process on Solid Sorbents

Model type	Sorbents	Condition	Expression
Power law model	Li_2ZrO_3	T: 550–600°, P_{CO_2}: 0.3–1 atm	$\frac{d\alpha}{dt} = kC^n_{CO_2}(1-\alpha)$
Power law model	CaO (3 mm)	T: 650–750°C, independent of P_{CO_2}	$\frac{d\alpha}{dt} = k\left(1-\alpha/\alpha_u\right)^2$
Power law model	Li_4SiO_4	T: 530–575°C, P_{CO_2}: 0.05–1 atm	$\frac{d\alpha}{dt} = Kf(p_{CO_2})(1-\alpha)^2$
Double exponential model	Li_4SiO_4, $Li_{3.85}Na_{0.15}SiO_4$	T: 460–600 °C, CO_2 :60–200 mL/min	$y = A\exp^{-k_1 t} + B\exp^{-k_2 t} + C$
Double-shell model	Li_2ZrO_3	T: 500–650°C, CO_2: 160 mL/min	$\frac{\Delta w}{w} = \frac{44\rho}{\rho_0}(1-y^3)$
Boltzmann equation (rapid reaction stage)	CaO-based (60–80 μm)	T: 500–650°C, P_{CO_2} : 0.15–0.25 atm	$\alpha = k_1 - k_1/(1+\exp((t-b)/c))$
Avrami-Erofeev equation (diffusion stage)	CaO-based (60–80μm)	T: 500–650°C, P_{CO_2}:0.15–0.25 atm	$\alpha = 1-\exp(-kt^n)$

that has a good agreement with the kinetic data, assuming that the CO_2 reaction and lithium diffusion processes occur during the CO_2 sorption process on Li_4SiO_4. According to this model, the whole process is controlled by the diffusion process once the lithium diffusion occurred.

Assuming that the O^{2-} diffusion in the ZrO_2 shell is the rate-limiting step, Lin et al. built a more detailed double-shell model to describe the process of CO_2 sorption on Li_2ZrO_3 at 500–650°C based on the double-shell mechanism proposed by Ida and Lin.[20] This mechanism shows that, during the sorption process, CO_2 reacts with Li_2ZrO_3 on the surface to form a double-shell structure consisting of ZrO_2 and Li_2CO_3 first. Then the sorption rate begins to decrease because Li^+, O^{2-}, and CO_2 have to diffuse through the ZrO_2 and Li_2CO_3 shells to react with each other. They also studied the mechanism of the desorption reaction.[21] It was found that Li_2CO_3 reacts with ZrO_2 on the interface to form Li_2ZrO_3 and CO_2. When the Li_2ZrO_3 forms a dense shell covering the unreacted ZrO_2, the desorption process continues with the diffusion of Li^+ and O^{2-} through the solid Li_2ZrO_3 shell and CO_2 through the liquid Li_2CO_3 to the outside. It has been mentioned that the double-shell mechanism is suitable for the CO_2 sorption/desorption process on Li_4SiO_4, as well.[22] However, the kinetic behaviors of this mechanism have not been analyzed.

The kinetic behavior of the CO_2 sorption process on CaO-based materials at 500–650°C and CO_2 partial pressure of 0.15–0.25 atm was analyzed by dividing the whole process into the rapid reaction and diffusion control stages. The Boltzmann and Avrami–Erofeev models were applied for the two stages, respectively.[23]

In summary, the power law model has the advantage of simplicity. However, it lacks the mechanism and deals with a rather narrow temperature range. The double exponential model agrees quite well with the experimental data, but the sorption–desorption balance reached during the sorption process has not been analyzed using this model. Moreover, the double-shell mechanism is suitable for the sorption process, but it must be supported by a relative kinetic model. Finally, the Avrami–Erofeev model associated with the reaction mechanism of the formation and growth of product crystals is a promising model for the sorption process. However, the kinetic model for the CO_2 desorption process on Li_4SiO_4 has not been reported yet.

Therefore, a suitable model combined with a detailed reaction mechanism in a wide temperature range is necessary for the industrial research and process design of CO_2 sorption/desorption. In this work, FactSage5.0 was used to analyze the theoretical composition of the CO_2 sorption/desorption reaction at different temperatures and atmospheres. Then, the SCM, double exponential, and Avrami–Erofeev models were developed, and their results were compared with the thermogravimetric (TG) experimental data. Finally, the sorption–desorption mechanism was illustrated using the suitable model, including the effects of steam on the sorption process.

Experimental

Characterization

The commercial Li_4SiO_4 (99.9% metal basis) was purchased from Alfa (Alfa Aesar). The material was treated at 750°C for 6 h before being used in the kinetic experiments.

The sample was identified by X-ray diffraction (XRD). A diffractometer (RIGAKU D/MAX 2550 VB/PC, Japan) coupled to a copper-anode X-ray tube was used. The K_α wavelength (1.54056 nm) was selected with a diffracted beam monochromator. Li_4SiO_4 was identified by the corresponding Joint Committee on Powder Diffraction Standards (JCPDS) in virtue of MDI Jade 5.0 software. The surface structure and particle size of the sample was characterized by scanning electron microscopy (SEM; JEOL JSM-6360LV, Japan).

A SDT Q600 Simultaneous Thermal Analyzer (TGA/differential scanning calorimetry (DSC)) was used to analyze the reversibility of CO_2 uptake, temperature ranges and kinetic behaviors of the CO_2 sorption/desorption process.

A WRT-3P TG equipment was modified to make sure that the steam will be conducted into the system continuously with CO_2 and N_2, as shown in Figure 1. The total flow rate was controlled at 100 mL/min using flow meter. The humidity controller consisted of an external water bath and an internal water bubbler. The H_2O concentration was controlled by the temperature of water bath and detected in the inlet of the balance. The influence of CO_2 dissolution in the water bubbler was negligible.

Sorption/desorption process

The CO_2 sorption/desorption temperature range and equilibrium conversion were confirmed first by calculating the

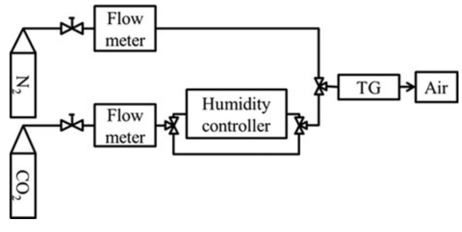

Figure 1. Schematic diagram of CO_2 sorption process.

Table 2. Experimental Conditions for the CO_2 Sorption/Desorption Process on Li_4SiO_4

Step	Condition
Heating up	Atmosphere: N_2 Gas flow rate: 100 mL/min Temperature: room temperature $\rightarrow$ adsorption temperature (10°C/min)
CO_2 sorption	Atmosphere: $N_2 \rightarrow CO_2$ Gas flow rate: 100 mL/min Temperature: adsorption temperature (550–700°C)
Process shift	Atmosphere: CO_2 Gas flow rate: 100 mL/min Temperature: adsorption temperature $\rightarrow$ desorption temperature (10°C/min)
CO_2 desorption	Atmosphere: $CO_2 \rightarrow N_2$ Gas flow rate: 100 mL/min Temperature: desorption temperature (650–750°C)

thermodynamic equilibrium of the sorption/desorption process via Gibbs free energy minimization using FactSage 5.0, which is widely used in the metallurgy field. The Li_4SiO_4 sample was heat treated using a thermogravimetric analyzer (TGA) from room temperature to 1000 °C with a heating rate of 10°C/min and gas flow rate of 100 mL/min to confirm the calculated results. The kinetics of the CO_2 sorption/desorption in the pure Li_4SiO_4 sample was examined using a TGA/DSC under the conditions listed in Table 2.

Results and Discussion

Figure 2 shows the XRD patterns of the prepared Li_4SiO_4 sample. It was fitted to JCPDS file 37-1472, and only the highly crystalline structure of Li_4SiO_4 was presented.

Figure 3 shows a micrograph of the Li_4SiO_4 sample, having a very smooth surface and a mean diameter of 25 μm. This characteristic shows that Li_4SiO_4 can be considered as a nonporous material, as proven by studies using nitrogen adsorption–desorption isotherms.[16] This result shows that the SCM may be used to describe the CO_2 sorption process on Li_4SiO_4.

Sorption/desorption temperature range and reversibility of CO_2 uptake

Figure 4a shows the thermodynamic results of the CO_2 sorption process on Li_4SiO_4 under pure CO_2. The process can be split into four stages according to the reactions at different temperatures, which are listed in Table 3.

When the temperature is higher than 724°C, only Li_4SiO_4 and CO_2 exist, indicating a desorption process. Theoretically, Li_4SiO_4 can totally react with CO_2 in the first three stages with different products at different temperature ranges (Figure 4a). Thus, the mass uptake of Li_4SiO_4 can be increased by improving the sorbent properties of Li_4SiO_4 when its conversion is lower than 100%.

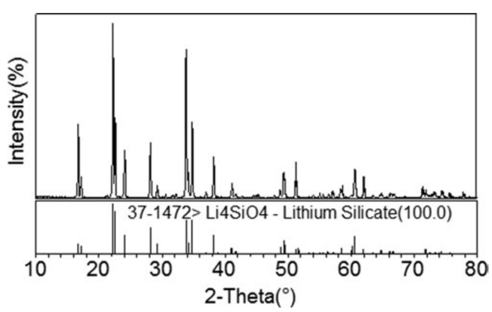

Figure 2. XRD pattern of the Li_4SiO_4 sample.

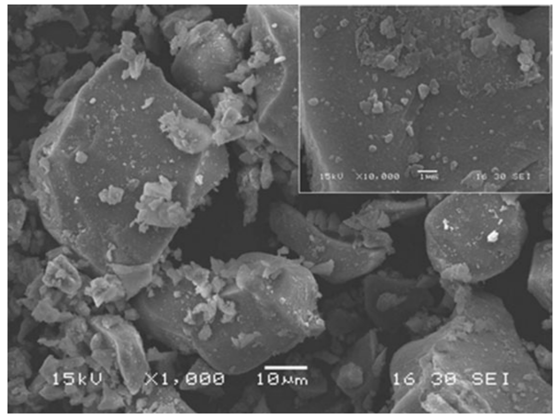

Figure 3. SEM images of the Li_4SiO_4 sample.

The thermoanalytical curve in Figure 5 was obtained by heating the Li_4SiO_4 sample in the CO_2 atmosphere with a heating rate of 10°C/min. A 1% decrease can be observed at 180–450°C because Li_4SiO_4 can react with steam at room temperature and dehydroxylation occurs when the temperature is higher than 180°C.[1,24] The weight increase of the sample with temperature is associated with the carbonation process when the temperature is higher than 450°C. Then, a sorption–desorption balance is achieved at 715°C, with a mass uptake of 30.56%. The desorption process occurs beyond 715°C.

The minimal sorption temperature obtained in the current experiment was 450°C, quite higher than the calculated value. This result can be attributed to kinetic limitation. Researchers from Toshiba proved that the Li_4SiO_4 weight increase at room temperature in ambient air is approximately 30% after 500 h mainly because of the CO_2 sorption.[1] The maximal experimental sorption temperature is 715°C, which is lower than the calculated value (723°C). However, this result may be caused by an experimental error. Thus, the temperature range for the sorption process is 450–723°C, and the sorption reaction mentioned below refers particularly to reaction (3). Hence, the reactants for the desorption process are Li_2CO_3 and Li_2SiO_3.

Figure 4b shows the thermodynamic results of the CO_2 desorption process in pure N_2. The CO_2 desorption reaction equation is given as follows according to the results

$$Li_2CO_3 + Li_2SiO_3 = Li_4SiO_4 + CO_2 \tag{4}$$

The CO_2 desorption reaction will not occur below 250°C, and the reaction conversion increases with temperature at 250–395°C. When the temperature is above 395°C, the theoretical conversion of the desorption reaction is 100%. Thus, the CO_2 desorption temperature ranges from 395 to 1000°C.

Figure 6 shows the reversibility of CO_2 uptake. This process was carried out at 700°C under pure CO_2 for 1 h and then under pure N_2 for 1.5 h in one cycle of sorption–desorption process. It can be seen that the maximal mass uptake of CO_2 for the first cycle is 33% and after 10 cycles of sorption–desorption process, it decreases to 31–32%. Obviously, the reversibility of CO_2 uptake is quite well. In our kinetic researches, the fresh Li_4SiO_4 was applied each time.

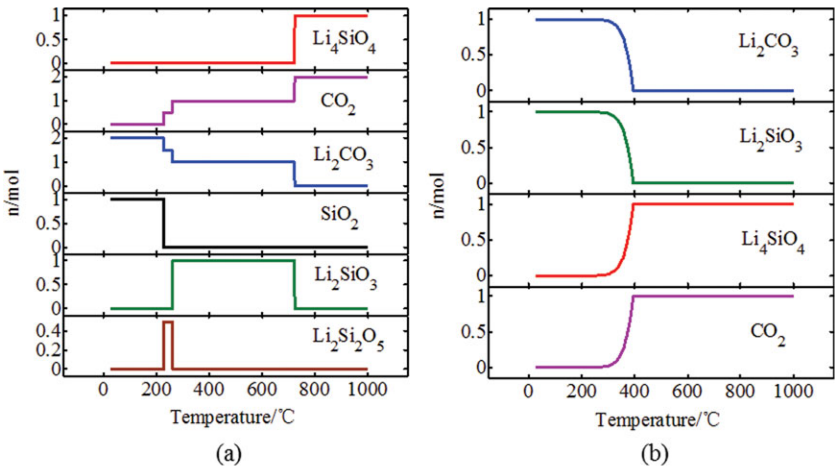

Figure 4. Thermodynamic equilibrium composition at different temperatures.

(a) Sorption process. (b) Desorption process (initial condition: Li_2CO_3:Li_2SiO_3:N_2 = 1:1:1000). [Color figure can be viewed in the online issue, which is available at wileyonlinelibrary.com.]

Kinetic analysis of CO_2 sorption/desorption on Li_4SiO_4

Considering the used temperature range of CO_2 sorption/desorption in Li_4SiO_4, the kinetic experiments for the sorption and desorption processes were performed at 550–700 and 650–750°C, respectively. The whole sorption/desorption process was divided into four steps, namely, the heating-up process, CO_2 sorption process, process shift, and CO_2 desorption process. The reaction conditions for each step are listed in Table 2.

Kinetic analysis of CO_2 sorption process without H_2O

Figure 7 shows the experimental results of the mass uptake of Li_4SiO_4 as it changes over time at different temperatures. When the temperature is lower than 650°C, the curves presented the same behavior. The mass uptake of Li_4SiO_4 for 300 min reaches 13.14, 13.60, 15.14, and 27.61% at 550, 575, 600, and 650°C, respectively, without showing a sorption–desorption balance. However, the curve obtained at 700°C shows a sharp increment within 15 min with a mass uptake of 33.77% before it reaches a sorption–desorption balance. The experimental data were used to analyze the following models.

Shrinking core model

The SCM, assuming that the reaction rate is controlled by the chemical reaction rate, is given as Eq. 5

$$d\alpha/dt = K(1-\alpha)^{2/3} \tag{5}$$

where α is the conversion of Li_4SiO_4, defined as q/q_{max}, q is the mass uptake of CO_2 per sorbent mass, q_{max} is the theoretical maximum of q found for Li_4SiO_4, which was 0.367 g of CO_2 per gram of sorbent according to the thermodynamic result, t is the time, and K is the kinetic constant.

Table 3. Reactions at the Different Temperature Ranges During the CO_2 Sorption Process on Li_4SiO_4

Temperature range (°C)	Stage	Reaction
25–228	1	$Li_4SiO_4 + 2CO_2 = 2Li_2CO_3 + SiO_2$
229–262	2	$2Li_4SiO_4 + 3CO_2 = 3Li_2CO_3 + Li_2Si_2O_5$
262–723	3	$Li_4SiO_4 + CO_2 = Li_2CO_3 + Li_2SiO_3$
724–1000	4	n.r.

This model is commonly used in nonporous materials. However, Figure 8a shows that Eq. 5 cannot fit the experimental data well at all temperatures.

Some authors have proposed an improved model, that is, with the exponential factor m changed from 2/3 to 2, to fit the experimental data well.[15] However, this model is not suitable for the experimental data in this work. Thus, the model with m varying from 0.1 to 10 was used to find the m that best agrees with the data. Some of the results at different temperatures are shown in Figure 8. Below 600°C, the data can only be fitted well if $m = 10$ when the conversion is larger than 0.2. At 650°C, the model can fit the experimental data when $m = 4$. However, when the temperature reaches 700°C, the expression cannot fit the data well regardless of the m value.

The results show that SCM cannot agree with the experimental data in the whole sorption temperature range, indicating that the sorption process is not simply controlled by the chemical reaction rate. A more complex model is necessary to simulate the whole process.

Double exponential model

The double exponential model is given in Eq. 6, which assumes that only two different processes take place during the CO_2 sorption process. These two processes are the CO_2 chemisorption process, which is produced directly by the sorption reaction on the surface of Li_4SiO_4, and the lithium diffusion process, which occurs once the carbonate-oxide external shell is completely formed

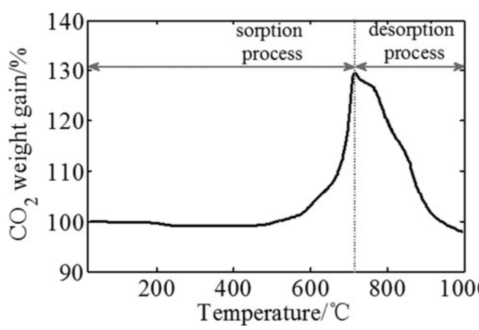

Figure 5. TG curves of Li_4SiO_4 obtained with a heating rate of 10°C/min in pure CO_2 atmosphere.

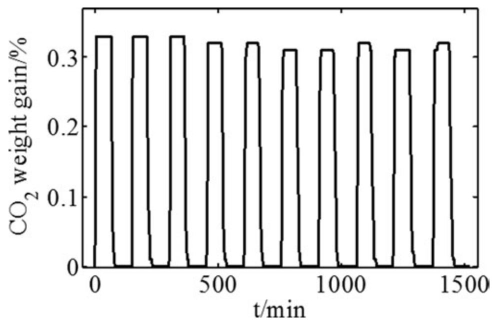

Figure 6. Experimental reversibility of CO_2 mass uptake on Li_4SiO_4 for 10 cycles of sorption–desorption process at 700°C (sorption process: pure CO_2; desorption process: pure N_2).

$$y = A\exp^{-k_1 t} + B\exp^{-k_2 t} + C \tag{6}$$

In Eq. 6, y is the weight percentage of chemisorbed CO_2, t is the time, and k_1 and k_2 are the exponential factors of the chemisorption and lithium diffusion process, respectively. A and B are the intervals at each process that controls the whole CO_2 sorption process, and C is the y-intercept.

Figure 9 shows that the double exponential model can fit the sorption kinetic experimental data well at different temperatures below 650°C in this work, but for the data obtained at 700°C, which reached a sorption–desorption balance at 15 min, the result is not so good as those of other temperatures.

The constants in the current model are listed in Table 4. k_1 is one order of magnitude larger than k_2 at each temperature below 650°C, demonstrating that the whole CO_2 sorption process is under the lithium diffusion control. k_2 increases with the temperature, reaches 1.97 E −3 at 700°C, which is one order of magnitude larger than the value at 650°C, and nearly equals k_1 at 700°C (1.98 E −3). The result shows that the lithium diffusion rate increases with temperature and has a sharp increment at 650–700°C. Thus, the whole sorption process is controlled both by the chemisorption and lithium diffusion rates. However, k_1 values at different temperatures are irregular.

According to the results, the limiting step of the whole sorption process is the lithium diffusion process, which is contradictory to the model assumption that the lithium diffusion process occurs when the carbonate-oxide external shell is completely formed. The process before formation of the

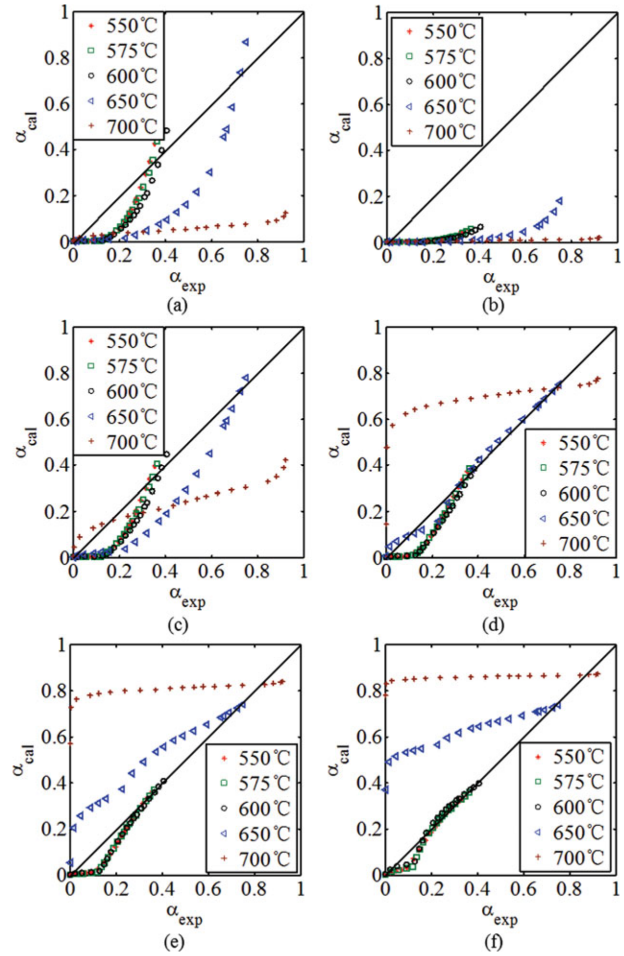

Figure 8. Relationship between calculated and experimental α values for *m*-order differential models (a) *m* = 2/3; (b) *m* = 1; (c) *m* = 2; (d) *m* = 4; (e) *m* = 6; (f) *m* = 10.

[Color figure can be viewed in the online issue, which is available at wileyonlinelibrary.com.]

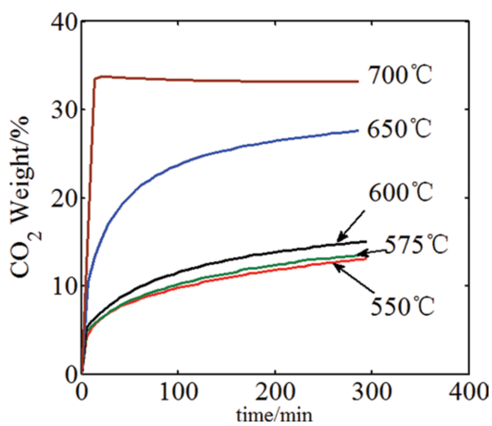

Figure 7. Change in mass uptake of Li_4SiO_4 over time at different temperatures with CO_2 pressure of 0.1 MPa.

[Color figure can be viewed in the online issue, which is available at wileyonlinelibrary.com.]

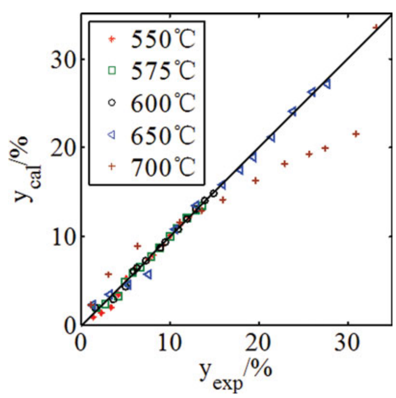

Figure 9. Relationship between calculated and experimental *y* values for double exponential model.

[Color figure can be viewed in the online issue, which is available at wileyonlinelibrary.com.]

Table 4. Kinetic Parameters of the Double Exponential Model for the Li_4SiO_4 Sample

Temperature (°C)	k_1 (s^{-1})	k_2 (s^{-1})	A	B	C	R_2
550	0.00407	0.00012	−5.76	−8.62	13.97	0.9956
575	0.0086	0.00014	−5.23	−9.28	14.19	0.9958
600	0.00851	0.00016	−5.62	−10.21	15.43	0.9957
650	0.00441	0.00026	−11.60	−16.51	27.35	0.9965
700	0.00198	0.00197	−19.79	−19.89	33.52	0.9622

external shell cannot be described and when the diffusion control stage occurred cannot be confirmed as well. Thus, the mechanism of the CO_2 sorption process is difficult to explain using the double exponential model. Moreover, this model cannot be used to simulate the sorption process because the temperature dependence of the parameters (A, B, and C) is not clear.

Avrami–Erofeev model

As shown in the XRD patterns (Figure 2), Li_4SiO_4 has a highly crystalline structure. The Avrami–Erofeev model, which is associated with the reaction mechanism of the formation and growth of reaction product crystals, has been used for reactants with highly crystalline structures.

The Avrami–Erofeev model is based on the typical model for gas–solid reactions

$$d\alpha/dt = KF(\alpha) \tag{7}$$

where

$$F(\alpha) = n(1-\alpha)[-\ln(1-\alpha)]^{(n-1)/n} \tag{8}$$

where α is the degree of conversion, K is the kinetic constant, n is the kinetic parameter, and t is the time. The temperature dependence of K is given by the following Arrhenius expression

$$K = K_0 \exp[-E/R(1/T - 1/T_0)] \tag{9}$$

Substituting Eq. 8 into Eq. 7 gives Eq. 10

$$\alpha = 1 - \exp(-kt^n) \tag{10}$$

where $k = K^n$

Taking the logarithm of Eq. 10 twice gives Eq. 11

$$\ln(-\ln(1-\alpha)) = \ln k + n \ln t \tag{11}$$

which is the equation of a straight line with slope n in the coordinates $\ln(-\ln(1-\alpha))$ vs. $\ln t$. The magnitude of n provides on the reaction rate, which is controlled by the rate of the formation and growth of the reaction product crystals when $n > 1$. If n is approximately 0.5, the reaction proceeds under the diffusion control.[25]

Figure 10a shows the ln $(-\ln(1-\alpha))$ vs. ln t line of the experimental data obtained in the CO_2 sorption process. Inflexion points are observed in the curves obtained below 650°C at 2 min with a Li_4SiO_4 conversion of approximately 0.1. Then, at 700°C, the inflection point became 11 min with a Li_4SiO_4 conversion of 0.84. The reaction reaches a sorption–desorption balance stage when the conversion reaches 0.92. Figures 10b,c show the linear fits of $\ln(-\ln(1-\alpha))$ on ln t for the two stages near the inflection point. All data can be fitted well, and the n and K for different stages can be obtained.

Figures 11a,b show the linear fits of the n value on the temperature for the first and second stages. The K values were fitted to the Arrhenius equation in Figures 12a,b. In the first stage, all slopes are larger than 1, indicating that the reaction is controlled by the rate of the formation and growth of the reaction product crystals. The active energy for this stage is 2.71 E +4 J/mol, implying a rapid reaction stage. In the second stage, the slopes are all approximately 0.3–0.4. This result means that the sorption process is under

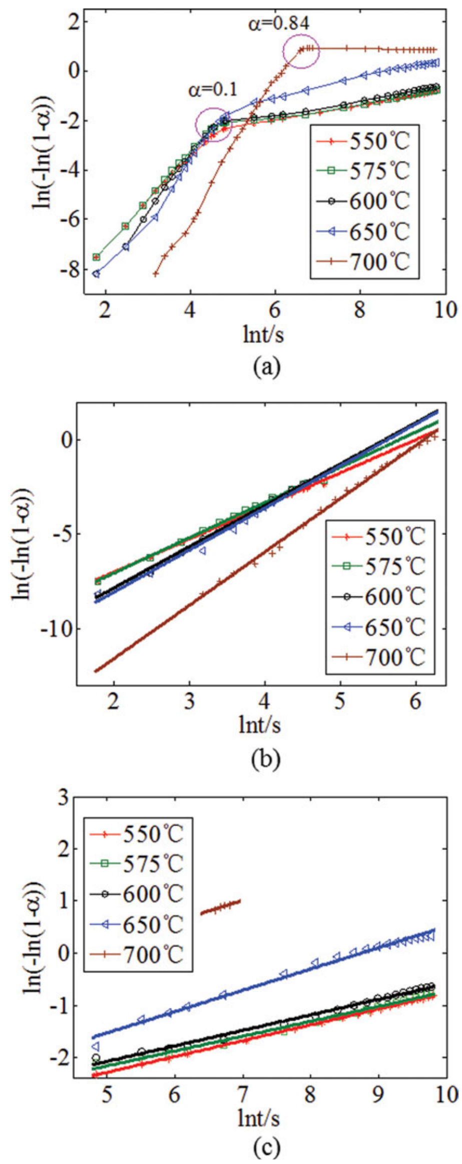

Figure 10. Fit of the CO_2 sorption kinetic experimental data with the (a) Avrami–Erofeev equation in the (b) first and (c) second stages.

[Color figure can be viewed in the online issue, which is available at wileyonlinelibrary.com.]

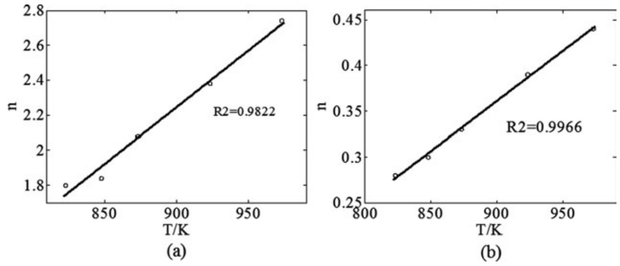

Figure 11. *n* value as a function of temperature in the Avrami–Erofeev model for the sorption process: (a) rapid reaction and (b) diffusion control stages.

the diffusion control, indicating a diffusion control stage. The active energy is increased to 2.72 E +5 J/mol, which is 10 times higher than that of the rapid reaction stage. The temperature dependence of n is given by Eq. 12

$$n = \begin{cases} 0.0065T - 3.6087 & \text{rapid reaction stage} \\ 0.0011T - 0.6259 & \text{diffusion control stage} \end{cases} \tag{12}$$

The Avrami–Erofeev model can agree with the experimental data well at each temperature. The whole process can be split into the rapid reaction and diffusion control stages according to n at the critical points of $\alpha \approx 0.1$ when the temperature is lower than 650°C and $\alpha = 0.84$ at 700°C. The rapid reaction stage is neglected in both the power law and double exponential models. The Avrami–Erofeev model can also be used in the simulation of the CO_2 sorption-enhanced fuel steam reforming process. Thus, this kinetic model is most suitable for the CO_2 sorption process on Li_4SiO_4.

Reaction mechanism of CO_2 sorption process on Li_4SiO_4

The reaction mechanism of the CO_2 sorption process on Li_4SiO_4 can be clearly described by the double-shell mechanism combined with the Avrami–Erofeev kinetic model. The whole desorption process involves the following procedures:

1. The CO_2 molecules react with Li_4SiO_4 to form solid Li_2CO_3 and Li_2SiO_3 nuclei on the surface. The reaction rate is controlled by the rate of the formation of the product crystals, and this procedure is very short.

2. The Li_2SiO_3 nuclei grow to form a shell covering the unreacted Li_4SiO_4, and then, Li^+ and O^{2-} have to diffuse through this Li_2SiO_3 shell to react with CO_2. The Li_2CO_3 nuclei form another shell outside the Li_2SiO_3 shell, and CO_2 molecules have to diffuse through it for the reaction to take place. Thus, the double shell is formed, and the diffusion process occurs in this step. The reaction rate is controlled by the formation and growth of the product crystals.

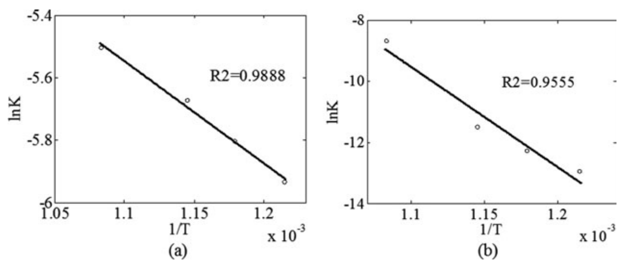

Figure 12. Plots of ln *K* vs. 1/*T* for the desorption process: (a) rapid reaction and (b) diffusion control stages.

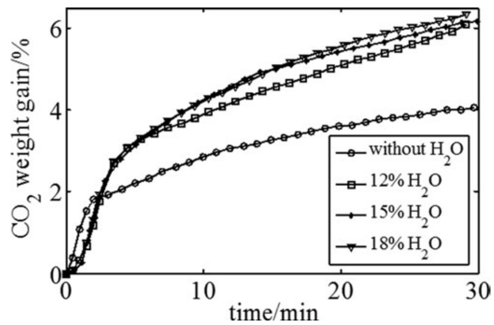

Figure 13. Change in mass uptake of Li_4SiO_4 over time at atmosphere with/without water at 575°C and total pressure of 0.1 MPa.

3. The thickness of the double shell increases with the reaction. When the diffusion resistance is large enough, the reaction rate rapidly decreases, and the reaction proceeds under the diffusion control. This step proceeds when $t > 2$ min ($\alpha > 0.1$) below 650°C and when $t > 11$ min ($\alpha > 0.84$) at 700°C.

The difference at 700°C can be attributed to the diffusion rate increase. The sorption process is controlled by chemical reaction rate until the Li_4SiO_4 conversion reaches 84.23%, when the diffusion resistance is large enough to control the process. It is also found that the initial kinetics is fast followed by a slow CO_2 uptake and then the kinetics become slow when the temperature is lower than 650°C. Therefore, how to improve the sorption properties should be the future work, such as doping of Li_4SiO_4 with hetero elements (Al, K, or Fe) to improve its CO_2 uptake in the rapid reaction stage or designing an easy-regeneration reactor. Meanwhile, the water in the methane steam reforming system was thought to have positive effect on the CO_2 sorption process on Li_4SiO_4. Thus, the water effect was investigated in the following secession.

Effect of steam on the CO_2 sorption Kinetics

The influence of steam on the CO_2 sorption process was analyzed in the gas with H_2O concentration of 12–18% at 575°C in a modified WRT-3P TG equipment. The result was shown in Figure 13. It can be seen that with the addition of steam, the CO_2 mass uptakes increase 60% more than without steam after 30-min adsorption. With the steam amount increasing, the adsorbent capture ability is enhanced accordingly. However, when the steam amount is greater than 15%, the effects of the steam amount on the sorption process is not obvious.

The sorption process with and without steam was analyzed using Avrami–Erofeev model. The kinetic parameters were summarized in Table 5. As it can be seen, the inflexion between rapid reaction stage and diffusion control stage is 1 min in dry CO_2 atmosphere and increased to 3 min by addition of water. In the rapid reaction stage, the n value is all about 1.8–2, which indicates the CO_2 sorption reaction is controlled by the formation of the product crystals. The K value is 2.64 E −3 in pure CO_2 atmosphere and decreased first by steam addition. However, with the increase of steam amount, the reaction rate increases when the H_2O concentration is lower than 15% and then decreases with H_2O concentration increasing. It is found that the effect of steam in the

Table 5. Parameters of Avrami-Erofeev Model for the CO_2 Sorption Process at 575°C With/Without Water

		Rapid reaction stage			Diffusion control stage		
Water content (%)	Inflexion point (min)	n	K	R_2	n	K	R_2
0	1	1.86	2.64 E −03	0.9880	0.36	1.51 E −06	0.9979
12	3	1.86	1.33 E −03	0.9998	0.38	5.99 E −06	0.9920
15	3	1.97	2.04 E −03	0.9812	0.39	7.46 E −06	0.9951
18	3	1.96	1.53 E −03	0.9985	0.42	1.07 E −05	0.9990

rapid reaction stage is not obvious. In the diffusion control stage, the n value and the reaction rate K value increase with the H_2O concentration. The reaction rate is 1.07 E −5 when the water composition is 18%, which is 10 times larger than the value obtained in the dry CO_2 atmosphere, which means the reaction rate in the diffusion control stage enhanced with steam addition.

For the steam effects on the CO_2 sorption kinetics can be summarized as follows[13]:

(a) Hydrolysis

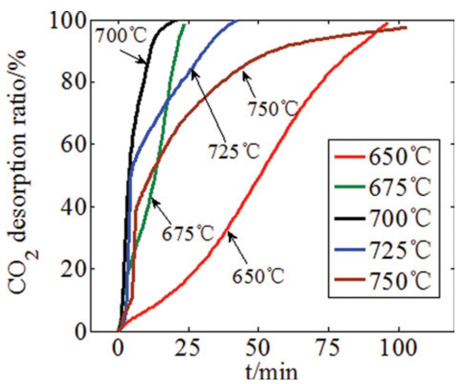

Figure 14. Change in CO_2 desorption ratio with time at different temperatures in pure N_2.

[Color figure can be viewed in the online issue, which is available at wileyonlinelibrary.com.]

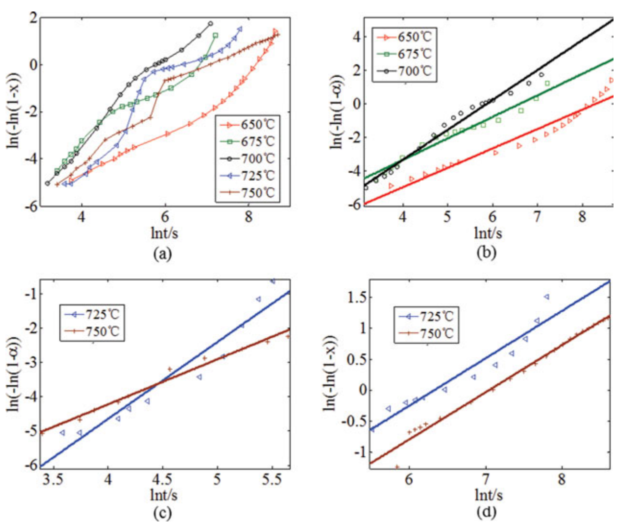

Figure 15. Fit of the CO_2 desorption kinetic experimental data with the (a) Avrami–Erofeev equation in the (b, c) first and (d) second stages.

[Color figure can be viewed in the online issue, which is available at wileyonlinelibrary.com.]

$$CO_2 + H_2O \leftrightarrow HCO_3^- + H^+ \leftrightarrow CO_3^{2-} + 2H^+ \tag{13}$$

$$Li_2O + H_2O \leftrightarrow 2Li^+ + 2OH^- \tag{14}$$

(b) Reaction

$$2Li^+ + CO_3{}^{2-} \leftrightarrow Li_2CO_3 \tag{15}$$

$$2H^+ + 2OH^- \leftrightarrow 2H_2O \tag{16}$$

(c) Total reaction

$$Li_2O + CO_2 \leftrightarrow Li_2CO_3 \tag{17}$$

The presence of steam is believed to enhance the mobility of Li and, therefore, the rate of the reactions, which is the reason that the steam effect on the diffusion control stage is more obvious than the rapid reaction stage and make the adsorption rate in diffusion control stage increased with the H_2O concentration. On the other hand, the formed Li_2CO_3 shell,

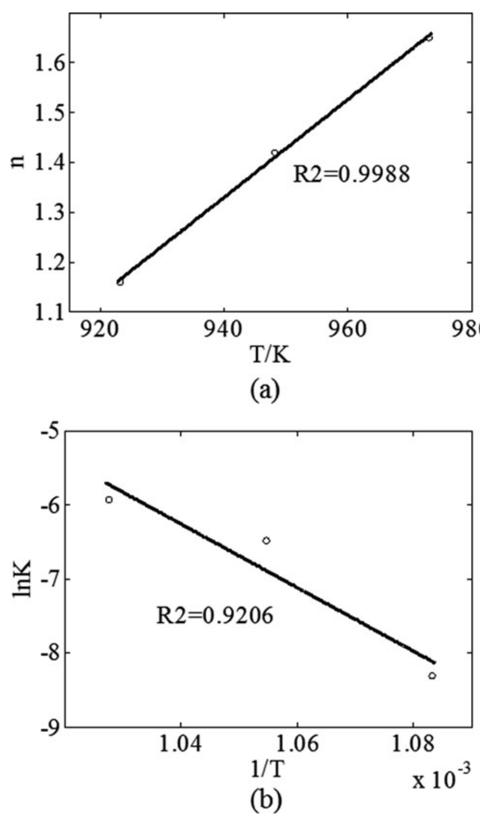

Figure 16. Kinetic parameters of the Avrami–Erofeev equation for the desorption process: (a) n vs. T line; (b) ln K vs. 1/T line.

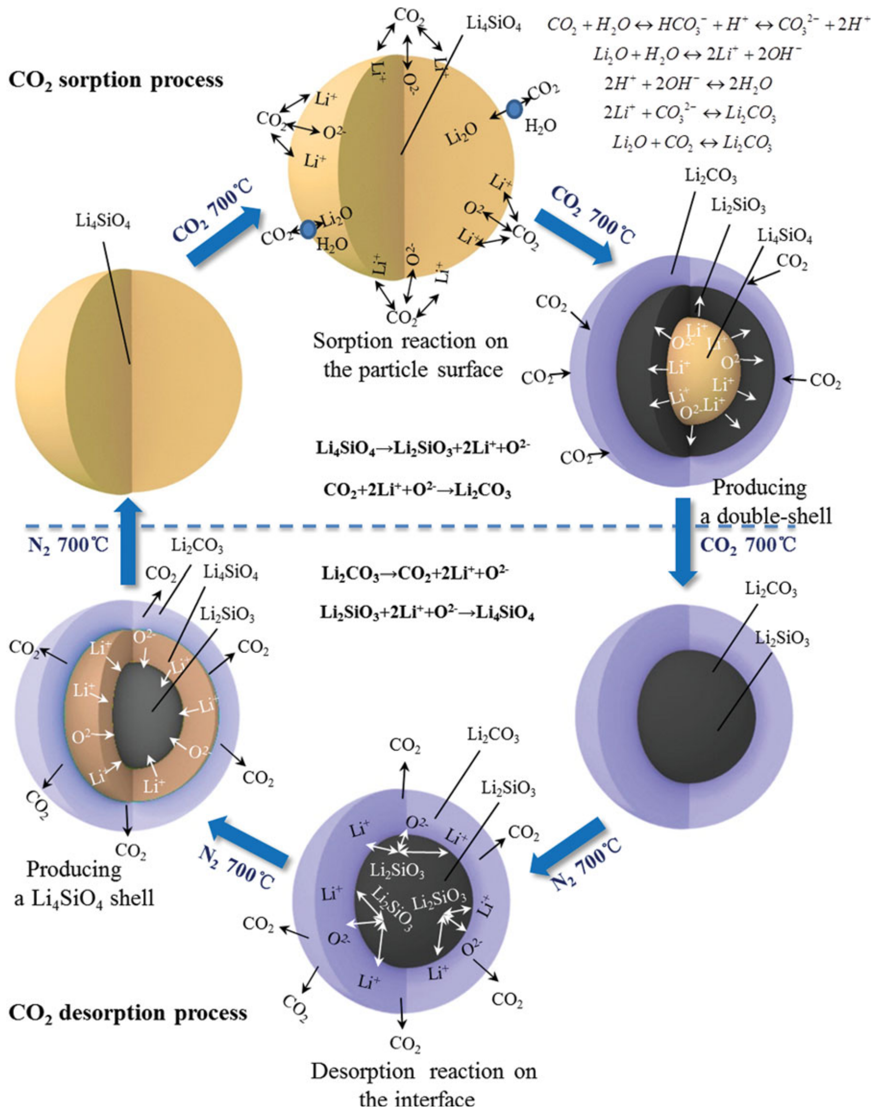

Figure 17. Illustration of double-shell mechanism for the CO_2 sorption/desorption process on Li_4SiO_4.

[Color figure can be viewed in the online issue, which is available at wileyonlinelibrary.com.]

which is on the surface of the adsorbent particle, is slightly dissolved in water with the solubility of 1.31 g Li_2CO_3/100 g H_2O and then the absorption is also promoted.[26] Thus, the inflexion point increased from 1 to 3 min.

Kinetic analysis of CO_2 desorption process on Li_4SiO_4

Pure N_2 was used in the CO_2 desorption process. Figure 14 shows the CO_2 desorption ratio as a function of time at 650–750°C. When the temperature is lower than 700°C, the reaction rate increases with the temperature. At 650°C, the CO_2 desorption ratio is 90.31% after 100 min. However, with the temperature increase, the ratio nearly reaches 100% after 24 and 21 min at 675 and 700°C, respectively. At temperatures higher than 725°C, the reaction rate decreases with temperature, compared with the rate at 700°C. The CO_2 desorption ratio is approximately 100% after 43 min at 725°C and reaches 97.12% in 100 min at 750°C. Thus, a desorption temperature near 700°C should be chosen to maintain a relatively high reaction rate. All the experimental data were applied to analyze the kinetic model for the CO_2 desorption process as follows.

Kinetic analysis of CO_2 desorption process

The Avrami–Erofeev model was also used to analyze the CO_2 desorption process. Figure 15a shows the $\ln(-\ln(1-x))$ vs. $\ln t$ line of the experimental data obtained in the CO_2 desorption process. The curves are nearly straight below 700°C, but at 725 and 750°C, the two processes have inflection points of approximately 5 min, as shown by the slope. The two curves are split into two stages at 5 min to analyze the kinetic behavior in detail. Figures 15b,c,d show the linear fit at different temperatures, and the n and K values were obtained according to the fitting results.

Figure 16a shows the linear fit of n as a function of temperature. Below 700°C, the slopes are all greater than 1 and increase with the temperature. This result means that the whole desorption process is controlled by the reaction rate of the formation and growth of the product crystals. The temperature dependence of n when the temperature is below 700°C is given by Eq. 19

$$n = 0.0098T - 7.8639 \tag{19}$$

Figure 16b shows the fitting of the K values with the Arrhenius equation when the temperature is below 700°C and the active energy is 3.57 E +5 J/mol, which is approximately 13 times larger than that of the rapid reaction stage in the CO_2 sorption process. As shown in the figure, the formation and growth of the product crystals is more difficult in the desorption process than in the sorption process.

When the temperature reaches 725°C, the slope n in the first stage has values of 2.25 and 1.32 for 725 and 750°C, respectively. These values indicate that the CO_2 desorption process is controlled by the formation and growth of the product crystals. In the second stage, both n values decrease to 0.76, indicating that the reaction proceeds under the diffusion control. This phenomenon is caused by the liquefaction of Li_2CO_3 considering that its melting point is 723°C. The liquefied Li_2CO_3 comes in full contact with Li_2SiO_3, the process is first controlled by the rate of the formation and growth of the product crystals. With the CO_2 formation, the gas assembles on the surface of Li_2SiO_3 because it hardly diffuses through the liquid film and the contact area of the reactants decreases. Thus, in the second stage, the CO_2 desorption process will proceed under the diffusion control.

The Avrami–Erofeev model is also suitable for the CO_2 desorption process. A desorption temperature near 700°C should be chosen to maintain a relatively high reaction rate. This kinetic model can be used to simulate the CO_2 sorption-enhanced fuel steam reforming process as well when the desorption temperature is lower than 723°C (the melting point of Li_2CO_3).

Reaction mechanism of CO_2 desorption process

The CO_2 desorption temperature should be below the melting point of Li_2CO_3. Therefore, the reaction mechanism of the CO_2 desorption process below 723°C was mainly analyzed using the Avrami–Erofeev kinetic model in this work. The CO_2 desorption process has the following three procedures.

1. Li_2CO_3 reacts with Li_2SiO_3 on the interface to form the Li_4SiO_4 nuclei and CO_2.
2. CO_2 diffuses out of Li_2CO_3, and the Li_4SiO_4 nuclei grow to form a dense shell in the middle, covering the unreacted Li_2SiO_3.
3. The CO_2 desorption process proceeds with the diffusion of Li^+ and O^{2-} through the solid Li_4SiO_4 shell and CO_2 through the Li_2CO_3 shell.

In contrast to the sorption process, the whole CO_2 desorption process is controlled by the rate of the formation and growth of Li_4SiO_4 crystals. The active energy for the formation and growth of Li_4SiO_4 is 3.57 E +05 J/mol, which is much larger than that of the formation and growth of Li_2CO_3 and Li_2SiO_3.

Conclusion

This work aims to develop a suitable kinetic model for investigating the kinetic behaviors and reaction mechanism of the CO_2 sorption/desorption process on Li_4SiO_4.

SCM, the double exponential, and Avrami–Erofeev models were compared to investigate the CO_2 sorption process. According to the results, the Avrami–Erofeev model was found to be most suitable for the CO_2 sorption process on Li_4SiO_4 within a wide temperature range. It can describe the rapid reaction stage, which is neglected in the other two models. Moreover, the reaction mechanism can be explained using the Avrami–Erofeev model combined with the double-shell mechanism, and the Avrami–Erofeev equation is also suitable for analyzing the kinetic behavior of the CO_2 desorption process.

As a summary, the reaction mechanism for the CO_2 sorption–desorption process schematically illustrated in Figure 17. In the sorption process, the CO_2 molecules come into contact with the sorbents and rapidly react to form a double-shell structure consisting of Li_2CO_3 and Li_2SiO_3. Then, the reactants have to diffuse through the double shell to react with each other. First, the reaction rate is controlled by the formation and growth of the product crystals. With the increase in the double-shell thickness, the reaction proceeds under the diffusion control. The presence of steam is believed to enhance the mobility of Li^+ and, therefore, the rate of the reactions, therefore, the effects of steam on the rapid reaction stage is not obvious, whereas the reaction rate of the diffusion control stage are 10 times larger with 18% H_2O concentration than the value obtained in the dry CO_2 atmosphere, which indicates the possibility of CO_2 capture technology with Li_4SiO_4 for the steam existence system.

For the desorption process, the temperature should be near 700°C to maintain a relatively high reaction rate. During the process, Li_2CO_3 reacts with Li_2SiO_3 on the interface to form a dense shell in the middle covering the unreacted Li_2SiO_3. Then the CO_2 desorption process proceeds with the diffusion of Li^+ and O^{2-} through the solid Li_4SiO_4 shell and CO_2 through the Li_2CO_3 shell. The whole desorption process is controlled by the rate of the formation and growth of the Li_4SiO_4 crystals.

Acknowledgments

This work was financially supported by the National Natural Science Foundation of China (Grant No. 21176080), the Natural Science Foundation of Shanghai (Grant No. 09ZR1407600), and the Fundamental Research Funds for the Central Universities. The authors thank Mr. Qinghui Zhang for the help of ploting.

Notation

A = kinetic parameter
B = kinetic parameter
C = kinetic parameter
b = kinetic parameter
c = kinetic parameter
E = active energy, J mol^{-1}
K = kinetic constant
k_1 = exponential factor for the chemisorption process, s^{-1}
k_2 = exponential factor for the lithium diffusion process, s^{-1}
$k = K^n$
m = kinetic parameter
n = kinetic parameter
q = mass uptake of CO_2 per mass of sorbent
q_{max} = the maximum mass uptake of CO_2 per mass of sorbent
T = temperature, K
t = time, s
w_0 = initial weight of Li_2ZrO_3 adsorbent, mg
w = weight gain of Li_2ZrO_3 adsorbent at time t, mg
y = weight percentage of CO_2 chemisorbed, %
y_1 = ratio of L to R_0

Greek letters

α = conversion of Li_4SiO_4, defined as q/q_{max}
ρ = molar density of ZrO_2, mol cm^{-3}
ρ_0 = mass density of Li_2ZrO_3, g cm^{-3}

Subscript

max = maximum of the variable

Literature Cited

1. Kato M, Yoshikawa S, Nakagawa K. Carbon dioxide absorption by lithium orthosilicate in a wide range of temperature and carbon dioxide concentrations. *J Mater Sci Lett*. 2002;21:485–487.

2. Reynolds PS. Carbon dioxide capture from flue gas by pressure swing adsorption at high temperature using a K-promoted HTlc: effects of mass transfer on the process performance. *Environ Prog*. 2006;25:334–342.
3. Barelli L, Bidini G, Gallorini F, Servili S. Hydrogen production through sorption-enhanced steam methane reforming and membrane technology: a review. *Energy*. 2008;33:554–570.
4. Beaver MG, Caram HS, Sircar S. Sorption enhanced reaction process for direct production of fuel-cell grade hydrogen by low temperature catalytic steam–methane reforming. *J Power Sources*. 2010;195:1998–2002.
5. Bhat SA, Sadhukhan J. Process intensification aspects for steam methane reforming: an overview. *AIChE J*. 2009;55:408–422.
6. Yang H, Xu Z, Fan M, Gupta R, Slimane R, Bland A, Wright I. Progress in carbon dioxide separation and capture: a review. *J Environ Sci*. 2008;20:14–27.
7. Hufton JR, Mayorga S, Sircar S. Sorption-enhanced reaction process for hydrogen production. *AIChE J*. 1999;45:248–256.
8. Koumpouras G, Alpay E, Lapkin A, Ding Y, Stepanek F. The effect of adsorbent characteristics on the performance of a continuous sorption-enhanced steam methane reforming process. *Chem Eng Sci*. 2007;62:5632–5637.
9. Lysikov A, Trukhan S, Okunev A. Sorption enhanced hydrocarbons reforming for fuel cell powered generators. *Int J Hydrogen Energy*. 2008;33:3061–3066.
10. Dou B, Dupont V, Rickett G, Blakeman N, Williams PT, Chen H, Ding Y, Ghadiri M. Hydrogen production by sorption-enhanced steam reforming of glycerol. *Bioresource Technol*. 2009;100:3540–3547.
11. Essaki K, Muramatsu T, Kato M. Effect of equilibrium shift by using lithium silicate pellets in methane steam reforming. *Int J Hydrogen Energy*. 2008;33:4555–4559.
12. Essaki K, Muramatsu T, Kato M. Effect of equilibrium-shift in the case of using lithium silicate pellets in ethanol steam reforming. *Int J Hydrogen Energy*. 2008;33:6612–6618.
13. Essaki K, Nakagawa K, Kato M, Uemoto H. CO_2 absorption by lithium silicate at room temperature. *J Chem Eng Jpn*. 2004;37:772–777.
14. Ochoa-Fernández E, Zhao TJ, Rønning M, Chen D. Effects of steam addition on the properties of high temperature ceramic CO_2 acceptors. *J Environ Eng*. 2009;135:397–403.
15. Ochoa-Fernández E, Rusten HK, Jakobsen HA, Rønning M, Holmen A, Chen D. Sorption enhanced hydrogen production by steam methane reforming using Li_2ZrO_3 as sorbent: sorption kinetics and reactor simulation. *Catalysis Today*. 2005;106:41–46.
16. Lee DK, Baek IH, Yoon WL. Modeling and simulation for the methane steam reforming enhanced by in situ CO_2 removal utilizing the CaO carbonation for H_2 production. *Chem Eng Sci*. 2004;59: 931–942.
17. Rusten HK, Ochoa-Fernández E, Lindborg H, Chen D, Jakobsen HA. Hydrogen production by sorption-enhanced steam methane reforming using lithium oxides as CO_2-acceptor. *Ind Eng Chem Res*. 2007;46:8729–8737.
18. Rodríguez-Mosqueda R, Pfeiffer H. Thermokinetic analysis of the CO_2 chemisorption on Li_4SiO_4 by using different gas flow rates and particle sizes. *J Phys Chem A*. 2010;114:4535–4541.
19. Venegas MJ, Fregoso-Israel E, Escamilla R, Pfeiffer H. Kinetic and reaction mechanism of CO_2 sorption on Li_4SiO_4: study of the particle size effect. *Ind Eng Chem Res*. 2007;46:2407–2412.
20. Xiong R, Ida J, Lin YS. Kinetics of carbon dioxide sorption on potassium-doped lithium zirconate. *Chem Eng Sci*. 2003;58: 4377–4385.
21. Ida JI, Lin YS. Mechanism of high-temperature CO_2 sorption on lithium zirconate. *Environ Sci Technol*. 2003;37:1999–2004.
22. Essaki K, Kato M, Nakagawa K. CO_2 removal at high temperature using packed bed of lithium silicate pellets. *J Ceramic Soc Jpn*. 2006;114:739–742.
23. Shi Q, Wu SF, Jiang MZ, Li QH. Reactive sorption-decomposition kinetics of nano Ca-based CO_2 sorbents. *J Chem Ind Eng*. 2009;60: 641–649.
24. Ortiz-Landeros J, Martínez-dlCruz L, Gómez-Yáñez C, Pfeiffer H. Towards understanding the thermoanalysis of water sorption on lithium orthosilicate (Li_4SiO_4). *Thermochim Acta*. 2011;515:73–78.
25. Zagorowsky GM, Prikhod'ko GP, Ogenko VM, Koval'chuk GK. Investigation of Kinetics of solid-phase synthesis of lithium orthosilicate. *J Thermal Anal Calorimetry*. 1999;55:699–705.
26. Essaki K, Kato M, Nakagawa K, Uemoto H. CO_2 Adsorption by lithium silicate at room temperature. *J Chem Eng Jpn*. 2004;37:772–777.

Manuscript received Nov. 3, 2011, revision received Mar. 29, 2012, and final revision received May 24, 2012.